

## RESEARCH ARTICLE

# Identification of a novel mechanism for meso-tetra (4-carboxyphenyl) porphyrin (TCPP) uptake in cancer cells

David J. Elzi<sup>1</sup> | William E. Bauta<sup>1</sup> | Jamila R. Sanchez<sup>1</sup> | Trisha Das<sup>1</sup> |  
 Shweta Mogare<sup>1</sup> | Peter Zannes Fatland<sup>1</sup> | Moises Iza<sup>1</sup> | Alexander Pertsemliadis<sup>2,3,4,5</sup> |  
 Vivienne I. Rebel<sup>1,3</sup>

<sup>1</sup>BioAffinity Technologies, Inc., San Antonio, TX, USA

<sup>2</sup>Department of Pediatrics, The University of Texas Health Science Center, San Antonio, TX, USA

<sup>3</sup>Department of Cell Systems & Anatomy, The University of Texas Health Science Center at San Antonio, San Antonio, TX, USA

<sup>4</sup>Greehey Children's Cancer Research Institute, The University of Texas Health Science Center at San Antonio, San Antonio, TX, USA

<sup>5</sup>Mays Cancer Center, UT Health San Antonio MD Anderson, San Antonio, TX, USA

## Correspondence

Vivienne I. Rebel, BioAffinity Technologies, 22211 West I-10, Suite 1206, San Antonio, TX 78257, USA.  
 Email: vr@bioaffinitytech.com

## Abstract

Porphyrins are used for cancer diagnostic and therapeutic applications, but the mechanism of how porphyrins accumulate in cancer cells remains elusive. Knowledge of how porphyrins enter cancer cells can aid the development of more accurate cancer diagnostics and therapeutics. To gain insight into porphyrin uptake mechanisms in cancer cells, we developed a flow cytometry assay to quantify cellular uptake of meso-tetra (4-carboxyphenyl) porphyrin (TCPP), a porphyrin that is currently being developed for cancer diagnostics. We found that TCPP enters cancer cells through clathrin-mediated endocytosis. The LDL receptor, previously implicated in the cellular uptake of other porphyrins, only contributes modestly to uptake. We report that TCPP instead binds strongly ( $K_D = 42$  nM) to CD320, the cellular receptor for cobalamin/transcobalamin II (Cbl/TCN2). Additionally, TCPP competes with Cbl/TCN2 for CD320 binding, suggesting that CD320 is a novel receptor for TCPP. Knockdown of CD320 inhibits TCPP uptake by up to 40% in multiple cancer cell lines, including lung, breast, and prostate cell lines, which supports our hypothesis that CD320 both binds to and transports TCPP into cancer cells. Our findings provide some novel insights into why porphyrins concentrate in cancer cells. Additionally, our study describes a novel function for the CD320 receptor which has been reported to transport only Cbl/TCN2 complexes.

## KEYWORDS

clathrin-dependent endocytosis, CD320, cell biology

## 1 | INTRODUCTION

Porphyrins are organic compounds with a basic structure of four pyrroles and, in some cases, a coordinated metal ion. Porphyrins have long been known to have an affinity for

neoplastic tissue,<sup>1</sup> which has led to their use in cancer diagnostics<sup>2-4</sup> and cancer therapeutics such as photodynamic therapy (PDT).<sup>5-7</sup> PDT causes cellular damage through the generation of oxygen radicals when photosensitizing agents are exposed to light.<sup>8</sup> The first porphyrin that was

**Abbreviations:** Cbl, cobalamin; CLTC, clathrin heavy chain; EGTA, ethylene glycol tetra-acetic acid; EIPA, ethyl-isopropyl amiloride; LDL, low-density lipoprotein; LDLR, low-density lipoprotein receptor; MES, 2-(*N*-morpholino) ethanesulfonic acid; TCN2, transcobalamin 2; TCPP, meso-tetra (4-carboxyphenyl) porphyrin.

approved as a photosensitizer in PDT for humans, porfimer sodium, was a mixture of porphyrins that also accumulated in healthy tissues; patients experienced the most severe side effects on their skin. The next-generation, laboratory-synthesized porphyrins, are single compositions and show an improved uptake in tumor tissue compared to skin, for example. They absorb long-wavelength light better than their older counterparts, which is critical for deeper tissue penetration. With the development of more focused and stable light sources, as well as flexible endoscopes, PDT has become a very successful and safe therapeutic approach for the treatment of non-melanoma skin cancers,<sup>9</sup> as well as obstructive biliary tract and lung cancers<sup>10,11</sup> and localized prostate cancer.<sup>6</sup> Furthermore, PDT shows great promise in the treatment of head and neck cancers<sup>12</sup> and cutaneous metastatic breast cancer.<sup>13-15</sup>

The modifications of porphyrins and porphyrin-like molecules that make them into desirable photosensitizers for PDT have been largely focused on properties of light absorption and tissue retention, without fully understanding how porphyrins and like molecules enter cells in the first place, and why some porphyrins, but not others, show a preference for tumor tissues. It has been shown that porphyrins can bind to low-density lipoproteins<sup>16-18</sup> and that the low-density lipoprotein receptor (LDLR) transports porphyrin-lipoprotein complexes into cells<sup>19-22</sup> through clathrin-mediated endocytosis.<sup>23,24</sup> Interestingly, cancer cells have increased uptake of lipoproteins,<sup>25</sup> possibly due to their increased metabolic needs.<sup>26</sup> Moreover, emerging evidence suggests that deregulated endocytosis is a characteristic of cancer cells.<sup>27,28</sup> It is thus conceivable that the selective uptake of porphyrins by cancer cells is in part due to increased LDLR internalization through an abnormally regulated endocytic process. However, some porphyrins show preferential uptake for one type of cancer over another,<sup>29</sup> indicating that a porphyrin's selectivity for tumors or healthy tissues is more complex than a single receptor and abnormally regulated endocytosis.

Our laboratory has been interested in the synthetic porphyrin meso-tetra (4-carboxyphenyl) porphyrin (TCPP). TCPP has been shown to accumulate in tumor cells<sup>30,31</sup> and is highly fluorescent,<sup>32</sup> which makes it an especially attractive agent for cancer diagnostics. As demonstrated by Patriquin et al in a clinical trial for the early detection of lung cancer in sputum cells, TCPP labeling of sputum cells can distinguish samples from high-risk patients with lung cancer from those without the disease with 81% accuracy.<sup>2</sup> Very little is known about the molecular basis of TCPP's tissue/tumor specificity, how TCPP enters cells, and where TCPP locates once in the cell. Hu et al have reported that cellular uptake of TCPP can be attenuated by general inhibitors of endocytosis, such as cold temperatures and hypertonic sucrose, but a more fundamental understanding is needed.<sup>33</sup> Elucidating

novel processes of cellular uptake can lead to TCPP modifications that may improve tumor specificity for diagnostic and/or therapeutic purposes.

Previous studies with other porphyrins have shown that tumor specificity may be related to the tumor microenvironment.<sup>34,35</sup> For simplicity, the current study focuses on the cancer cell itself, in particular on the question, "How does TCPP enter cancer cells?" We found that the mechanism of TCPP internalization occurs in part through clathrin-mediated endocytosis. While we confirmed a modest 10% contribution to this process by LDLR, CD320, the cellular receptor for vitamin B12 (Cobalamin; Cbl),<sup>36,37</sup> contributed nearly 40% to TCPP uptake in multiple cancer cell lines. This CD320-mediated uptake constitutes a novel mechanism for porphyrins to enter cancer cells.

## 2 | MATERIALS AND METHODS

### 2.1 | Cell lines and reagents

Lung cancer cell lines HCC15, H1993, H157, H358, H1395, and HCC2450 (The Hamon Center for Therapeutic Oncology Research at UT Southwestern Medical Center, Dallas, TX) and prostate cancer cell line LNCaP and breast cancer cell line MDA-MB-231 (ATCC, Manassas, VA) were grown in RPMI 1640 (GE-Hyclone, Logan, UT) supplemented with 10% fetal bovine serum (Sigma-Aldrich, St. Louis, MO), 50 units/mL penicillin, and 50 µg/mL streptomycin (Life Technologies, Grand Island, NY). Prostate cancer cell lines PC3 and DU145 and breast cancer cell line MCF-7 (ATCC), were grown in DMEM (GE-HyClone) supplemented with 10% fetal bovine serum and 50 units/mL penicillin and 50 µg/mL streptomycin. Trypsin-ETDA was obtained from Life Technologies (Carlsbad, CA). Accutase was obtained from Innovative Cell Technologies (San Diego, CA). Collagenase IV and dispase were obtained from STEMCELL Technologies (Vancouver, British Columbia, Canada). Unless specified elsewhere, all other chemicals were obtained from Sigma-Aldrich.

Cell lines were DNA fingerprinted through the McDermott Center Sequencing Core at UT Southwestern Medical Center using the PowerPlex Fusion system (Promega, Madison, WI) and confirmed against fingerprint libraries.

### 2.2 | Chemical inhibition of endocytosis and TCPP uptake

Cells were treated with the following chemical inhibitors of endocytosis: sucrose, filipin III (2 µg/mL) (Cayman Chemical, Ann Arbor, MI), ethylene glycol tetra-acetic acid (EGTA) (Research Products International, Mount Prospect, IL), rottlerin (Tocris Bioscience, Bristol, UK), ethyl-isopropyl

amiloride (EIPA), and chlorpromazine hydrochloride. Cells were incubated with these inhibitors for 10 minutes at room temperature before being assayed for TCPP uptake by flow cytometry as described.

### 2.3 | $K_D$ determination of CD320: TCPP interaction and inhibition of TCPP uptake by Cbl/TCN2

Serial dilutions of TCPP (from a TCPP stock solution of  $1.26 \times 10^{-3}$  M in water with  $4.76 \times 10^{-2}$  M sodium bicarbonate) were made in MES buffer (0.1 M, pH 6.1) containing 2 mM calcium chloride in molecular biology-grade water (HyClone) to reach a 10 nM TCPP solution. Human recombinant (r) CD320 (R&D Systems, Minneapolis, MN) was resuspended in 0.1 M MES buffer, pH 6.1, containing 2 mM calcium chloride and combined with equal volumes of the 10 nM TCPP solution described previously to achieve a final concentration of rCD320 from 0-70 nM and 5 nM of TCPP. The combined solution was incubated in a black 96-well plate (Corning Life Science, Corning, NY) in the dark for 1 hour at 21°C prior to fluorescence measurements. Fluorescence measurements were made using a Tecan Spark plate reader (Männedorf, Switzerland) with an excitation wavelength of 414 nm and fluorescence emission detected at 656 nm. Data were analyzed using GraphPad Prism software (San Diego, CA), as described in the Supplemental Material. For the transcobalamin II (TCN2) inhibitory studies, human rTCN2 (R&D systems) and Cbl were complexed at a ratio of 1:3 at 4°C for 2-4 hours as described.<sup>38</sup> The Cbl/TCN2 complex (8 µg/mL) was added simultaneously with the TCPP for the TCPP uptake assay in live cells.

### 2.4 | Immunofluorescence microscopy of CD320

HCC15 cells were grown on glass coverslips overnight and serum-starved for 1 hour before treatments. Cells were exposed to 0.1 M MES buffer with 2 mM calcium chloride with or without 9 µg/mL TCPP (Frontier Scientific, Logan, UT) or 33 µg/mL Cbl/TCN2 for 10 minutes. Cells were fixed in 4% paraformaldehyde prepared in Dulbecco's phosphate-buffered saline (DPBS) for 10 minutes at room temperature and permeabilized in 0.5% Triton-X in DPBS for 10 minutes at room temperature. Cells were immunostained with an anti-CD320 antibody (Proteintech, Chicago, IL) overnight at room temperature, followed by incubation with Alexa Flour 488-conjugated-anti-rabbit antibody (Thermo Fisher Scientific) for 60 minutes at room temperature. Coverslips were mounted in Anti-Fade

Diamond with DAPI (Thermo Fisher Scientific) and analyzed on an Olympus Microscope using a 40 × objective. Images were captured with cellSens software (Olympus Life Science, Waltham, MA).

### 2.5 | Lentivirus production and shRNA knockdown of LDLR and CD320 proteins

Lentivirus were prepared in 293T cells via calcium phosphate transfection with the Broad Consortium shRNA library clones as described.<sup>39</sup> The shRNA targeting sequences are as follows: human LDLR-46: GGGCGACAGATGCGAAAGAAA; human LDLR-48: ACATCAACAGCATCAACTTTG; human CD320-27: CCCTCAGAGACCTGAGCTCTT; human clathrin heavy chain -83: CCTGTGTAGATGGGAAAG AAT; human clathrin heavy chain-84: GCCAATGT GATCTGGAACCTTA; control shRNA: CGTGATCTTC ACCGACAAGAT. Two days after infection, cells were grown in a selection medium containing 2.5-5 µg/mL puromycin (Corning Life Sciences) for 2 more days, after which cells were harvested for flow cytometry and western blot analysis.

### 2.6 | TCPP uptake by flow cytometry

Cells were harvested by trypsinization and washed twice in DPBS.  $0.5$  to  $1 \times 10^6$  cells were added to 0.1 M MES buffer with TCPP and incubated at 37°C for 10-30 minutes. Cell labeling was stopped by placing cells on ice and immediately adding ice-cold DPBS. Cells were spun down and washed twice more in DPBS. The last wash step contained 2 µg/mL propidium iodide (Thermo Fisher Scientific) so dead cells could be excluded from the analysis. Cells were kept on ice until their analysis on the LSRII flow cytometer (BD Biosciences, San Jose, CA).

### 2.7 | Subcellular fractionation

Subcellular fractions were prepared from HCC15 cells using the Minute Plasma Membrane Protein Isolation and Cell Fractionation Kit (Invent Biotechnologies, Inc, Plymouth, MN) as per the manufacture's protocol. Prior to subcellular fractionation, HCC15 cells were serum-starved for 1 hour, followed by a 10-min exposure to 0.1 M MES buffer with 2 mM calcium chloride, with or without 9 µg/mL TCPP. Membrane fractions were solubilized in 30 mM Triton X-100 (Fisher Scientific, Waltham, MA) and 10.3 mM sodium dodecyl sulfate (Fisher Scientific) in PBS prior to the BCA protein concentration assay (Thermo Fisher).

## 2.8 | Western immunoblotting and antibodies

Whole cell lysates or subcellular fractions were separated by SDS-PAGE, and protein expression was analyzed by western immunoblotting as described.<sup>40</sup> The bands on the western blots were visualized by enhanced chemiluminescence (ECL) (GE-Amersham, Amersham, UK) and quantified by Li-COR Image Studio software (Li-COR Biosciences, Lincoln, NB). Antibodies used were anti-CD320 and anti-LDLR (Proteintech), anti-tubulin (Sigma-Aldrich), anti-GAPDH (Thermo-Fisher, Rockford, IL), anti-ATP1A1 (Novus Biologicals, Centennial, CO), anti-rabbit-IgG-HRP, and anti-mouse-IgG-HRP (both from Cell Signaling Technologies, Danvers, MA).

## 2.9 | In-cell ELISA assay for endocytosis activity

In-cell ELISA assays to quantify endocytosis activity in HCC15 cells were performed as previously described.<sup>41</sup> The antibodies used for uptake were biotin-labeled anti-transferrin receptor (clone OKT9, Thermo Fisher Scientific), biotin-labeled anti-CD44 (clone G44-26, BD Biosciences, San Jose, CA), and biotin-labeled anti-IGF1R (R&D systems). Streptavidin-HRP secondary antibody, HRP substrate detection reagents, and sulfuric acid were obtained from R&D systems and used per the manufacturer's instructions. When inhibitors of endocytosis were used in selected uptake assays, cells were incubated for 10 minutes at 37°C prior to the addition of the biotinylated antibody.

# 3 | RESULTS

## 3.1 | TCPP uptake by various cancer cell lines measured by flow cytometry

To determine the mechanism of TCPP uptake in cancer cells, we first developed a flow cytometry assay that would allow us to quantify cellular uptake of TCPP. As depicted in Figure 1A, HCC15 lung cancer cells exposed to increasing doses of TCPP show a dose-dependent increase in fluorescence intensity. An extensive dose range experiment, shown in Figure 1B, reveals a small but reproducible plateau from 9 to 11  $\mu\text{g}/\text{mL}$  TCPP. When HCC15 cells are exposed to 9  $\mu\text{g}/\text{mL}$  TCPP, the cellular uptake of TCPP occurs in a linear manner between 5 and 20 minutes after the onset of the exposure (Figure 1C). Based on these results, we selected 9  $\mu\text{g}/\text{mL}$  TCPP and 10 minutes labeling time for all subsequent experiments. A panel of lung cancer cell lines (Figure 1D), prostate cancer cell lines (Figure 1E), and breast cancer cell

lines (Figure 1F) show that all cancer cell lines take up TCPP, albeit at different levels.

TCPP labeling of cells was performed after the cells were dissociated from the plate by trypsin treatment. Trypsin is known to cleave peptides after C-terminal arginine and lysine residues.<sup>42</sup> To investigate whether trypsin treatment damages cell surface proteins important for TCPP uptake, we measured TCPP uptake in HCC15 and LNCaP cells after detachment by collagenase or dispase—both of which have different peptide cleavage specificities compared to trypsin<sup>43,44</sup>—or accutase, which is reported to be less harsh than trypsin for cell detachment<sup>45,46</sup> (Figures S1-S7). TCPP uptake was found to be similar for all dissociation methods investigated, which suggested that trypsinization does not specifically affect TCPP cell entry.

## 3.2 | TCPP is taken up by lung cancer cells by clathrin-mediated endocytosis

Endocytosis can occur through clathrin-dependent mechanisms, caveolin-dependent mechanisms, and caveolin-and-clathrin-independent mechanisms.<sup>47</sup> Early studies have shown that TCPP uptake in colon cancer cells was not inhibited when cells were treated with filipin, an inhibitor of caveolin-mediated endocytosis<sup>33</sup>; the other two endocytotic pathways were never tested directly. We wanted to confirm that the flow cytometry-based TCPP uptake assay would behave as expected when endocytosis was inhibited before we tested the role of clathrin-dependent and caveolin-and-clathrin-independent pathways in TCPP uptake. In order to do so, we treated a panel of lung cancer cell lines (HCC15, H157, and H358 cells) with hypertonic sucrose at 4°C temperature, conditions known to generally inhibit endocytosis,<sup>48,49</sup> and measured TCPP uptake in the flow cytometry assay. Figure 2A shows that in this assay hypertonic sucrose and cold treatment inhibited TCPP uptake similarly in all three cancer cell lines by approximately 60% and 90%, respectively. In addition, treatment of HCC15 and H157 cells with filipin III, an inhibitor of caveolin-dependent endocytosis, showed no effect on TCPP uptake (Figures S1-S7).<sup>33</sup>

To determine if TCPP was internalized through clathrin-dependent endocytosis, we used a known chemical inhibitor of this particular type of endocytosis, chlorpromazine.<sup>50</sup> When we compared TCPP uptake in HCC15 cells that were pretreated with different amounts of chlorpromazine, we observed that TCPP uptake was inhibited in a dose-dependent manner (Figure 2B), showing up to 80% inhibition at the highest chlorpromazine doses. Very similar effects of chlorpromazine were observed on TCPP uptake in two additional lung cancer cell lines, H157 and H358 (Figure 2C). Cell viability was not significantly changed with chlorpromazine treatment (Figures S1-S7) in any of the cell lines treated. To

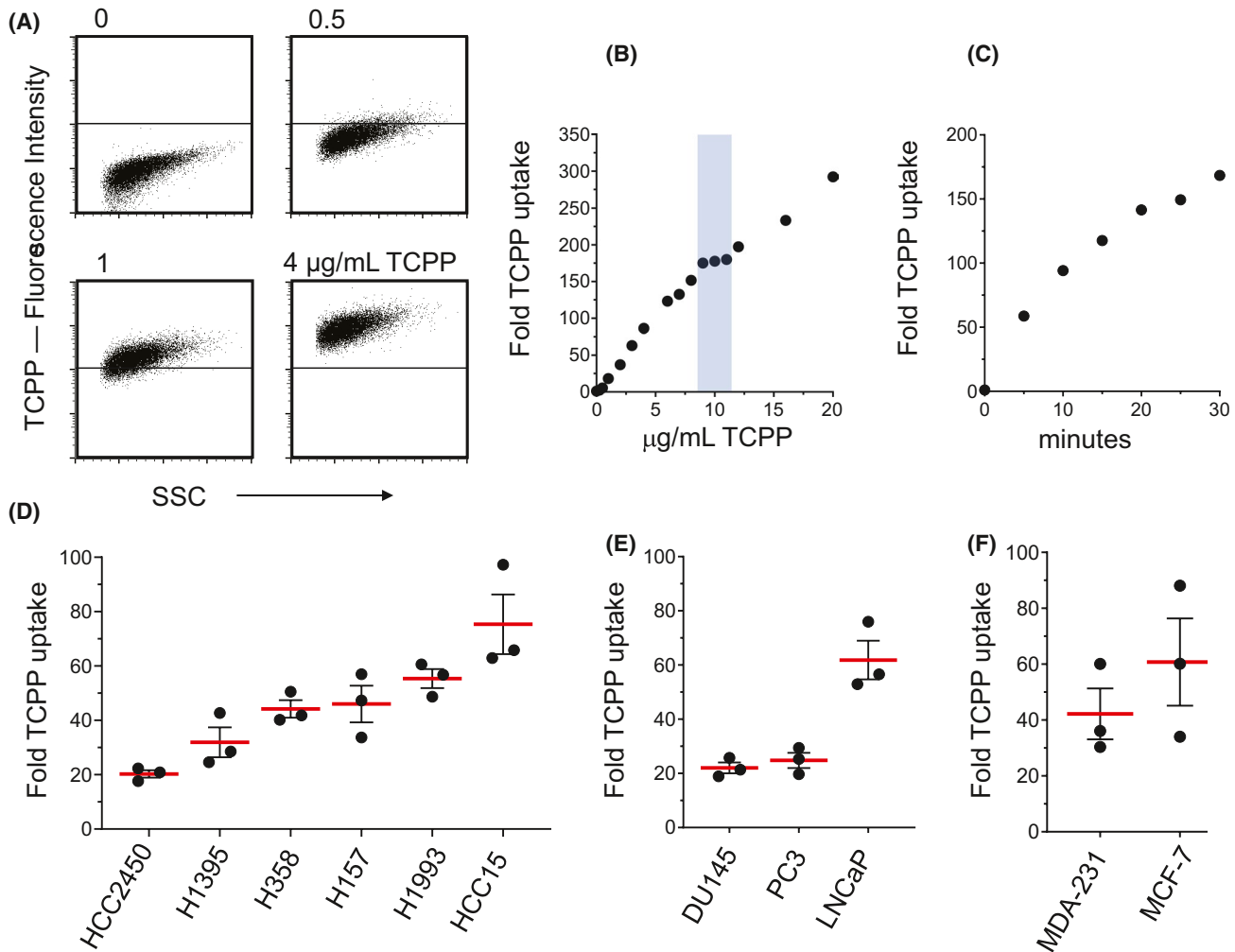


**FIGURE 1** TCPP uptake in cancer cell lines as measured by flow cytometry. A, Representative dot-plots of HCC15 cells stained with 0, 0.5, 1, and 4 µg/mL TCPP for 30 minutes. B, Concentration-dependent TCPP uptake. HCC15 cells were stained with TCPP (0–20 µg/mL) for 30 minutes. The TCPP fold uptake is calculated by dividing the average fluorescent intensity of stained TCPP cells by the average fluorescent intensity of unstained cells. The shaded box indicates the reproducible labeling plateau. The data are representative of three experiments. C, Time-dependent TCPP uptake. HCC15 cells were stained with 9 µg/mL TCPP for 0–30 minutes. The data are representative of three experiments. D, TCPP uptake in lung cancer; E, prostate cancer; and F, breast cancer cell lines. Shown are values of individual experiments (black bullets), the average value (red bar), and the SEM (black bars)

confirm the role of clathrin in the endocytosis-mediated uptake of TCPP, we knocked down endogenous clathrin heavy chain (CLTC) in HCC15 cells by shRNA. TCPP uptake in these CLTC knockdown cells was reduced compared to that in cells with intact levels of CLTC. However, the reduction in TCPP uptake after CLTC knockdown was much less than what was observed with chlorpromazine at the highest dose tested (Figures S1–S7).

To evaluate the contribution of caveolin-and-clathrin-independent endocytosis on TCPP uptake, we used macropinocytosis inhibitors EIPA and rottlerin in HCC15 and H157 cells<sup>51–53</sup> (Figures S1–S7). EIPA only inhibited TCPP uptake by 15% in H157 cells at the highest concentration tested, while HCC15 cells were unaffected. Rottlerin did not inhibit TCPP uptake in either cell line.

These data suggest that TCPP enters cells through clathrin-mediated endocytosis and not through caveolin-dependent or caveolin-and-clathrin-independent endocytotic pathways.

### 3.3 | Low-density lipoprotein receptor (LDLR) expression does not correlate with TCPP uptake in cancer cells

Previous LDLR studies implicated the interactions between LDLR and porphyrin-lipoprotein complexes as an avenue for porphyrin uptake in cancer cells.<sup>19–22</sup> We hypothesized that decreasing LDLR activity would inhibit TCPP uptake. To test this, we employed lentivirus-delivered shRNAs to knock-down endogenous LDLR in HCC15 cells (Figure 3A). TCPP

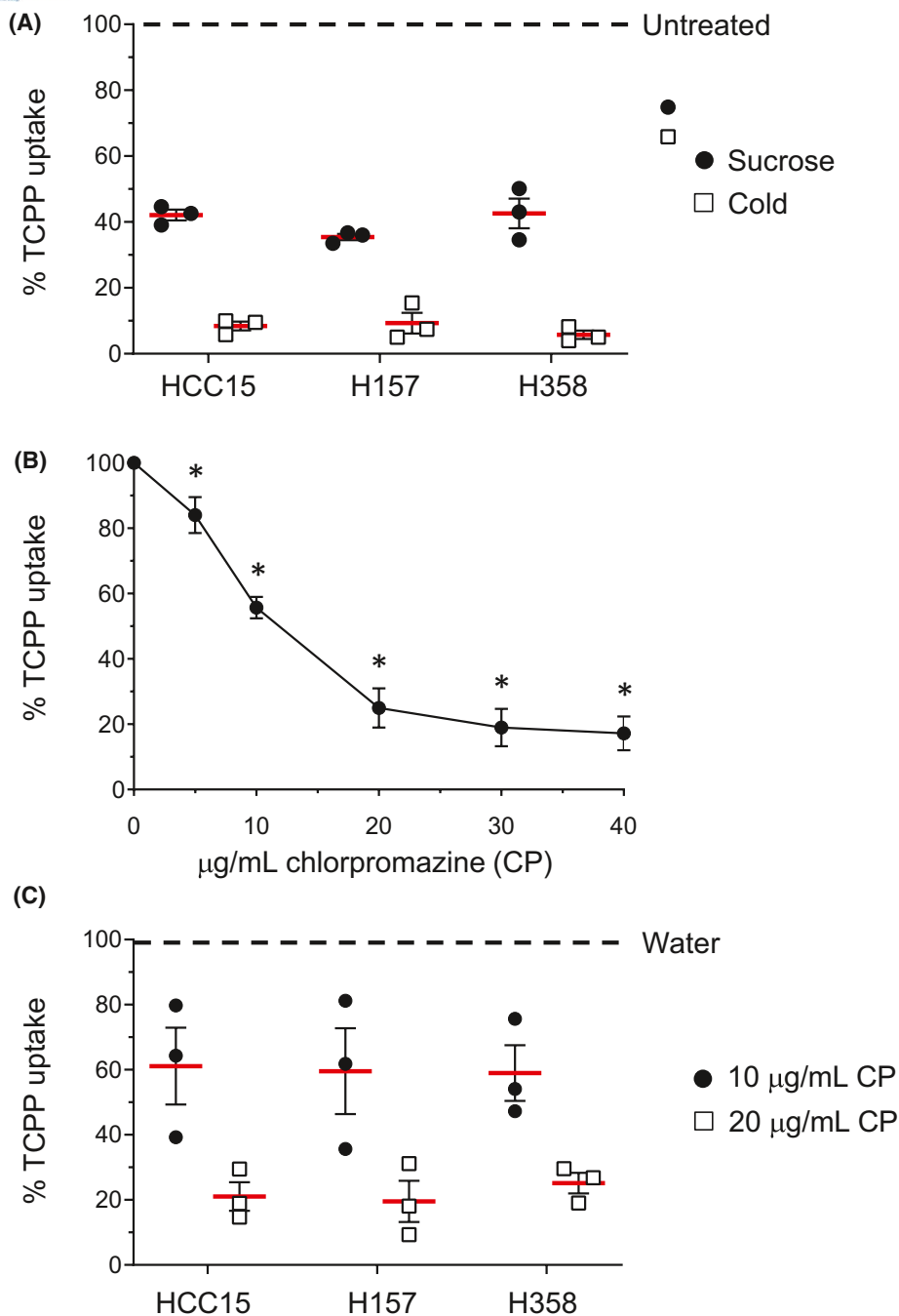


**FIGURE 2** TCPP enters live cells by endocytosis. A, TCPP uptake in lung cancer cells is inhibited by sucrose and cold temperature (4°C). Black bullets represent individual experiments, the red bar the average value, and the black bars the SEM. All average values differ significantly ( $P < .05$ ) from untreated cells, which was arbitrarily set at 100% (dashed line). B, TCPP uptake in HCC15 lung cancer cells is inhibited by chlorpromazine in a dose-dependent manner. Shown are the average values  $\pm$  SEM ( $n = 4$  or more),  $*P < .05$  compared to untreated control. C, TCPP uptake in HCC15, H157, and H358 lung cancer cells is inhibited by chlorpromazine. Shown are individual experiments (bullets), average (red bar), and the SEM (black bars). All average values differ significantly ( $P < .05$ ) from untreated cells, which was arbitrarily set at 100% (dashed line)

uptake was measured in these engineered HCC15 cells and compared to that of the parental HCC15 cells (Figure 3B). A modest reduction in TCPP uptake (5%-12%) was observed despite LDLR knockdown ranging from 63% to 84%. These data show that the LDLR plays a minor role in TCPP uptake and suggests that TCPP can enter the cell via alternative receptors.

### 3.4 | TCPP binds to CD320 and competes with Cbl/TCN2

While looking for candidate receptors that may be involved in TCPP cell entry other than LDLR, we focused on receptors with a domain structure analogous to that of LDLR and

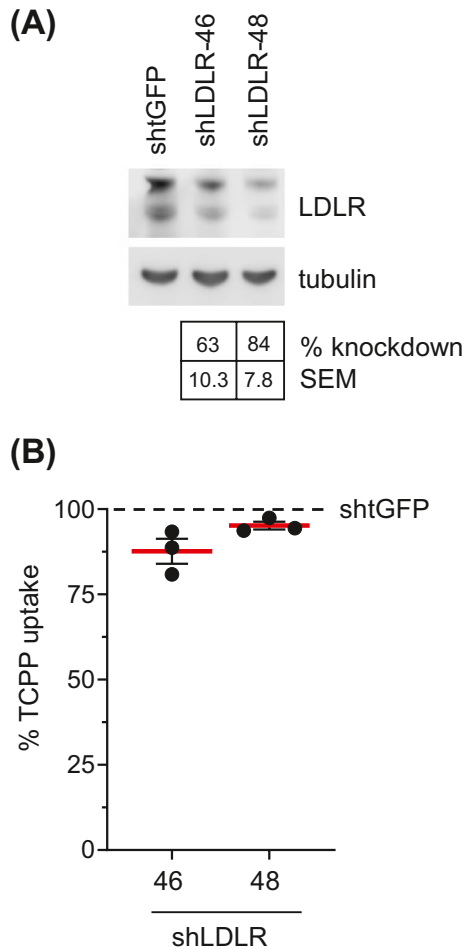


**FIGURE 3** LDLR contributes minimally to TCPP uptake. A, LDLR knockdown minimally affects TCPP uptake. Shown is a representative western blot of LDLR protein levels in HCC15 cells after infection with a lentivirus encoding a control shRNA directed at tGFP (shtGFP) or shRNA targeting LDLR (shLDLR-46 and shLDLR-48). Tubulin was used as a loading control. CD320 and tubulin protein levels were quantified by the western blots; CD320 was normalized to tubulin. The CD320 knockdown was determined relative to the GFP control, which was arbitrarily set at 100%. The boxes below the western blot show the average CD320 knockdown  $\pm$  SEM for each cell line above ( $n = 3$ ). (B) Percent TCPP uptake after LDLR knockdown (using two different viral constructs) is presented for three individual experiments (black bullets). TCPP uptake was calculated relative to shtGFP control cells (dashed line), which was arbitrarily set at 100%. Both LDLR knockdown constructs significantly ( $P < .05\%$ ) reduced TCPP uptake compared to the shtGFP control, albeit at low levels

that was considered to be internalized by clathrin-mediated endocytosis. This led us to CD320. CD320 is a receptor that internalizes Cbl when bound to its chaperone protein, TCN2. Interestingly, Cbl is a corrin that shows structural similarity to porphyrins including TCPP. We hypothesized that TCPP uses CD320 for cell entry. We first investigated whether there is a direct interaction between TCPP and CD320. Porphyrin binding to proteins generally is accompanied by

a change in porphyrin fluorescence intensity until maximum binding (saturation) is achieved.<sup>54-60</sup> Therefore, the binding of TCPP to CD320 was studied by measuring the relative fluorescence of TCPP at a single concentration (5 nM) in the presence of variable concentrations of rCD320. The excitation wavelength was set at TCPP's absorbance maximum of 414 nm, and fluorescence intensity was measured at its fluorescence maximum (656 nm). Neither rCD320 nor the buffer had significant fluorescence under these conditions, and thus the fluorescence of the mixtures was entirely attributable to free and protein-bound TCPP. Previous studies indicated that TCPP does not aggregate under the conditions of the experiment (W. Bauta, unpublished results).<sup>61</sup> Fluorescence values were normalized by dividing the fluorescence intensity of each well by the maximum fluorescence intensity—the fluorescence of TCPP solution with no added rCD320—for the run. TCPP fluorescence intensity decreased in a sigmoidal fashion as a function of the added CD320 concentration (Figure 4A). Modeling of these data indicated cooperative binding of multiple TCPP molecules to rCD320 with an apparent dissociation constant ( $K_D$ ) of approximately 42 nM (Supporting Information).

The binding data only suggest *in vitro* binding of TCPP to CD320. Therefore, it is important to examine if TCPP interacts with CD320 under physiological conditions. Specifically, we wanted to determine if the Cbl/TCN2 complex competes for TCPP uptake in live cells as measured by flow cytometry. The results of this experiment, depicted in Figure 4B, show that even a conservative amount of the Cbl/TCN2 complex (8  $\mu\text{g}/\text{mL}$ ) was able to partially inhibit TCPP uptake in all three cancer cell lines tested.

### 3.5 | CD320 is a candidate receptor for TCPP

We next set out to determine if CD320 internalizes upon exposure to TCPP. HCC15 cells were grown on coverslips and exposed to TCPP, Cbl/TCN2, or MES buffer alone. The coverslips were fixed so that immunocytochemistry could be performed for the CD320 protein. As shown by Figure 5A, CD320 staining was observed at the cell membrane and diffused through the cell before the addition of TCPP. After TCPP exposure, CD320 staining was diminished from the cell membrane. This was confirmed by subcellular fractionation experiments (Figure 5B). The staining pattern is different from the observed localization of CD320 after exposure to Cbl/TCN2. Under similar conditions, CD320 staining showed strong punctate dots after Cbl/TCN2 exposure.

Lastly, it is known that the binding activity of CD320 to its ligands requires calcium.<sup>62-64</sup> We, therefore, tested if chelating calcium by EGTA affected TCPP uptake in HCC15 cells. Figure 5C shows that EGTA inhibits TCPP uptake in

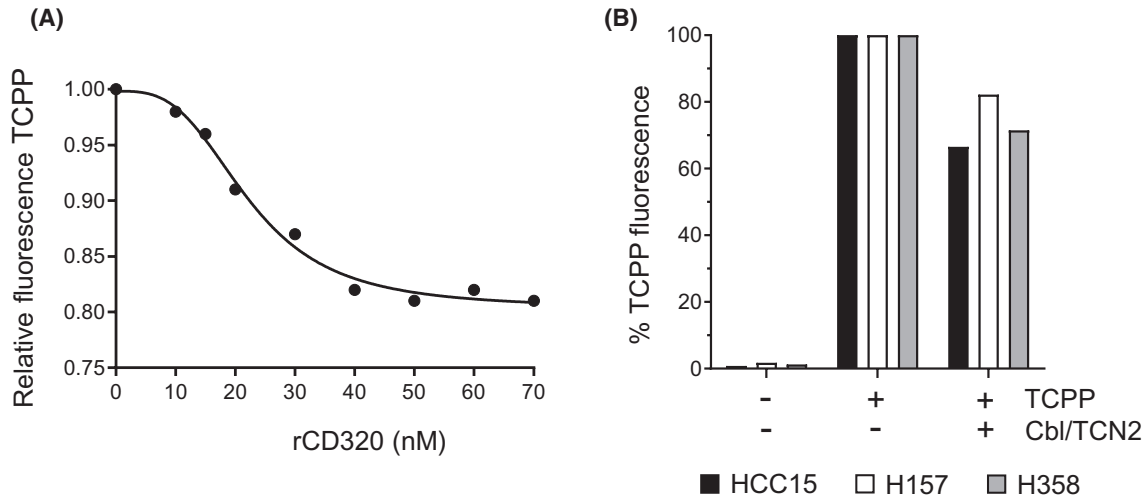


**FIGURE 4** TCPP binds to rCD320. A, Relative fluorescence of TCPP solutions as a function of the concentration of added rCD320. Relative fluorescence values were calculated as the ratio of the TCPP fluorescence at a given rCD320 concentration divided by the maximum fluorescence of TCPP in the absence of rCD320. The circles represent average values of two to five experiments. B, The addition of 4  $\mu$ g of Cbl/TCN2 complex reduced TCPP uptake in HCC15, H157, and H358 lung cancer cells as measured by flow cytometry. Values are normalized to TCPP uptake in the absence of Cbl/TCN2

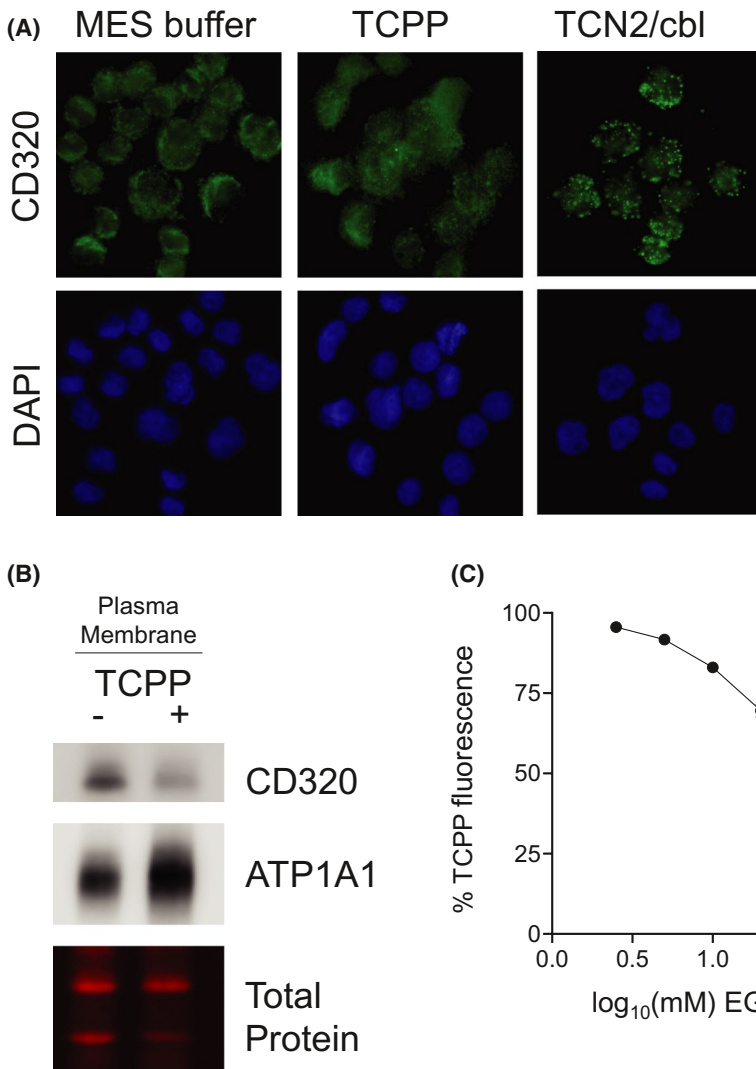


**FIGURE 5** TCPP induces internalization of CD320. A, CD320 localization is altered upon TCPP or Cbl/TCN2 exposure in HCC15 cells. Anti-CD320 antibody (green) or DAPI (blue-nuclear stain) images are shown. Figures are representative of three independent experiments. B, CD320 protein levels in HCC15 cells are reduced at the plasma membrane after TCPP exposure. ATP1A1 serves as an independent plasma membrane marker. C, TCPP uptake in HCC15 cells is reduced with the addition of EGTA. Values are normalized to 0 mM EGTA. Shown are means from three independent experiments  $\pm$  SEM. Of note: the high concentration range of EGTA used in this set of experiments is the result of the acidic pH under which the TCPP uptake assays are performed (pH 6.1). In this milieu, EGTA is less efficient as a calcium chelator<sup>99,100</sup>

a dose-dependent manner. This observation provides further support for a functional interaction between CD320 and TCPP.

### 3.6 | CD320 knockdown inhibits TCPP uptake in multiple cancer cell lines

The previous experiments provided evidence for a strong interaction between TCPP and CD320, suggesting that abrogating endogenous CD320 expression in live cells would decrease TCPP uptake. Endogenous CD320 was knocked down in HCC15, H157, and H358 cells by lentivirus-delivered shRNAs. Western blot analysis of CD320 protein demonstrated 85%–96% knockdown of CD320 in shCD320-treated cells compared to cells treated with a control shRNA (Figure 6A). TCPP uptake was measured to determine the direct contribution of CD320 protein to TCPP uptake in live cells. TCPP uptake was inhibited 39% in HCC15 cells and 11% in H157, compared to cells infected with a lentivirus encoding a control shRNA directed against the GFP protein (Figure 6B). TCPP uptake was not affected in H358 cells upon knocking down CD320.

Similar results were observed in prostate and breast cancer cell lines. Figure 7A shows that CD320 protein levels were reduced by approximately 80%–95% as compared to controls. TCPP uptake was inhibited in a subset of these CD320 knockdown cells: 30% in LNCaP cells, 21% in DU145 cells, and 39% in MDA-MB-231 cells (Figure 7B). TCPP uptake was not affected in PC3 or MCF-7 cells upon knocking down CD320.

To ensure specificity of shCD320 knockdown on TCPP uptake, we identified an additional shRNA sequence to CD320, which effectively reduced CD320 protein levels; HCC15 cells treated with this alternative shRNA showed similar effects on TCPP uptake inhibition (Figures S1–S7). In addition, we demonstrated that the rate of clathrin-dependent endocytosis was not affected by CD320 knockdown (Figures S1–S7).

Taken together, these results identify CD320 as a novel receptor used for TCPP uptake in cancer cells.

## 4 | DISCUSSION

Despite recent advances in the use of porphyrins in cancer diagnostics and therapy, the mechanism of why porphyrins accumulate in cancerous versus non-cancerous tissue is still poorly understood. The current study was undertaken to gain a better understanding of how porphyrins are taken up by cancer cells. In order to measure porphyrin uptake, we developed a flow cytometric assay in which cells were exposed to 9  $\mu\text{g}/\text{mL}$  of TCPP for 10 minutes. This concentration is

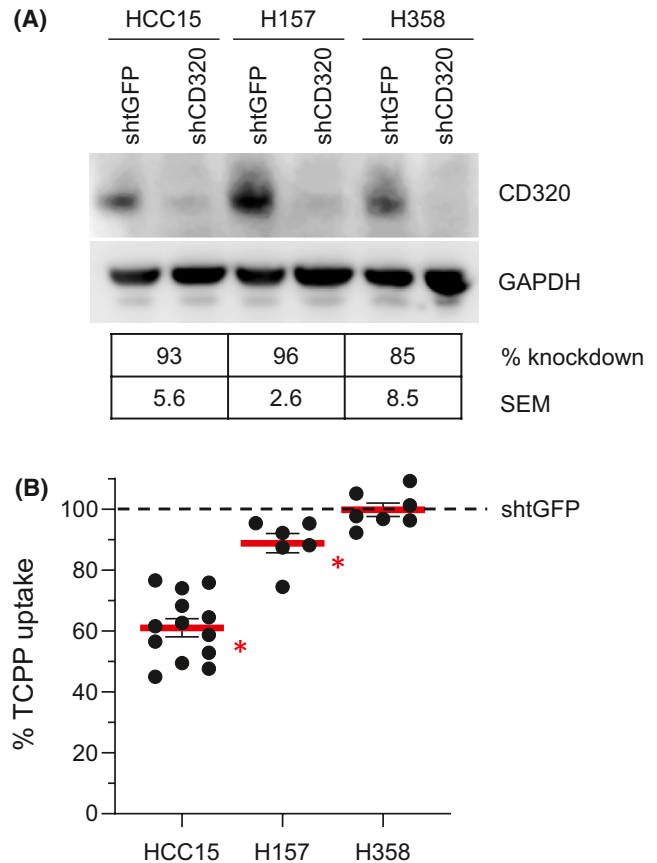


**FIGURE 6** Reduction of CD320 inhibits TCPP uptake in lung cancer cell lines. A, Lentivirus-mediated CD320 knockdown reduced CD320 protein levels as measured by the western blot. A representative western blot of CD320 and GAPDH (loading control) is shown. CD320 and GAPDH protein levels were quantified, and CD320 protein levels were normalized to GAPDH. The CD320 knockdown was determined relative to the GFP control, which was arbitrarily set at 100%. The boxes below the western blot show the average CD320 knockdown  $\pm$  SEM for each cell line above ( $n = 3$ ). B, TCPP uptake is inhibited in two out of three lung cancer cell lines upon knockdown of CD320. Bullets represent values of individual experiments, the red bar the average, and the black bars the SEM. The average TCPP uptake in HCC15 cells and H157 cells after CD320 knockdown differs significantly ( $*P < .05$ ) from the shGFP control, which was arbitrarily set at 100% (dashed line)

similar to that used for a flow cytometry-based test using TCPP to detect early-stage lung cancer in sputum samples (manuscript in preparation).

We confirmed the findings of earlier studies that caveolin-independent endocytosis contributes significantly to TCPP uptake in cancer cells. In particular, we demonstrated that clathrin-dependent pathways play a role in TCPP uptake by two independent methods. While chemical inhibition of clathrin-mediated endocytosis resulted in an 80% reduction of TCPP uptake, knockdown of CLTC, an essential component of the clathrin complex, showed only a 20% reduction in TCPP uptake. This apparent discrepancy

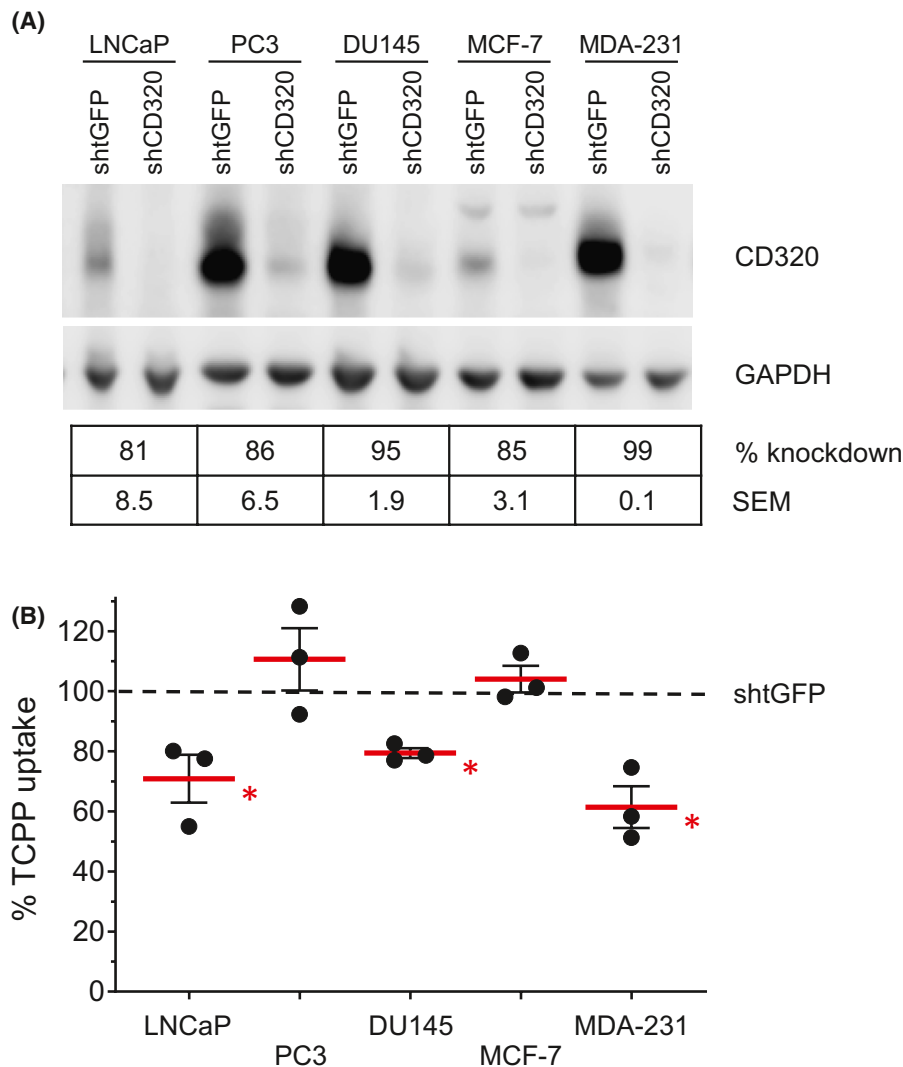


**FIGURE 7** Reduction of CD320 inhibits TCPP uptake in prostate and breast cancer cell lines. A, Lentivirus-mediated CD320 knockdown reduces CD320 protein levels as measured by the western blot. A representative western blot of CD320 and GAPDH (loading control) is shown. CD320 and GAPDH protein levels were quantified, and CD320 protein levels were normalized to GAPDH. The CD320 knockdown was determined relative to the GFP control, which was arbitrarily set at 100%. The boxes below the western blot show the average CD320 knockdown  $\pm$  SEM for each cell line above ( $n = 3$ ). B, TCPP uptake is inhibited in two out of three prostate cancer cell lines (LNCaP, DU145) and one of two breast cancer cell lines (MDA-231) after CD320 knockdown. Values of individual experiments are presented by the black bullets, the average value by the red bars, and the SEM by the black bars. The dashed black line represents the shtGFP control, which was arbitrarily set at 100%. \* $P < .05$ , compared to shtGFP control

in outcome between the two methodologies may be the result of incomplete CLTC knockdown since small amounts of the clathrin complex can still facilitate endocytosis.<sup>65,66</sup> Our results suggest that clathrin-and-caveolin-independent pathways do not contribute to TCPP uptake in the cell lines tested.

Porphyryns can bind LDL and other proteins in plasma such as albumin and HDL, as well as metals, which all could act as a porphyrin-carrier for cell entry,<sup>19-21,67</sup> facilitating endocytosis. Although not specifically ruled out, these factors are not likely to have played a role in the TCPP uptake assay presented in the current study since the experiments were performed in MES buffer, in the absence of serum and

with extensively washed cells. Moreover, the complexation of metals to porphyrins results in significant changes to the absorption and fluorescence emission spectra of the porphyrin,<sup>68,69</sup> which was not observed in our studies (W. Bauta, unpublished observations).

We could not establish that the LDLR plays a major role in TCPP uptake, despite previous studies implicating the importance of the LDLR in porphyrin uptake.<sup>19-22</sup> It is important to note that in these earlier studies porphyrins other than TCPP were used.<sup>19-22</sup> Moreover, Kongshaug et al showed that structurally different porphyrins have different affinities for LDLs.<sup>70</sup> More importantly, these authors also showed that a porphyrin's ability to bind to LDL does not correlate with its

ability to localize to tumors, which supports our findings that LDLR is only a minor facilitator of porphyrin uptake.

In the search for other cell surface molecules that enable porphyrins to enter cancer cells, we found that TCPP binds to CD320 with high affinity. CD320 mediates the uptake of TCPP in cancer cell lines derived from lung, prostate, and breast tissues, which constitutes a novel function for this receptor. CD320 was initially cloned from follicular dendritic cells as a molecule implicated for proper germinal center growth.<sup>71</sup> CD320 was subsequently found to be widely expressed in most tissues<sup>72</sup> and functionally characterized as the cellular receptor that facilitates cell entry of Cbl/TCN2 complexes.<sup>37,73</sup> CD320 surface expression increases upon cell proliferation, as Cbl is an essential co-factor for DNA synthesis.<sup>74,75</sup> Cancer cells, which have an increased demand for Cbl to meet their metabolic needs, were found to express higher levels of CD320 than their non-cancerous counterparts.<sup>76</sup> The increased expression of CD320 on cancer cells could thus contribute to the accumulation of TCPP in these cells.

The sigmoidal TCPP-rCD320 binding curve suggests cooperative binding of multiple TCPP molecules to CD320 with a surprisingly low  $K_D$ .<sup>77</sup> We speculate that multiple TCPP molecules bind the two LDLR type-A domains of CD320 in a cooperative manner. The spatial proximity of two TCPP molecules may explain the observed decrease in fluorescence intensity upon binding. TCPP aggregation at the binding site of CD320 is quite possible and might be facilitated by the proximity of modular LDL binding motifs at that binding site, but examining this scenario would require further study.

Both CD320 and LDLR contain LDLR-A1 and LDLR-A2 ligand-binding domains.<sup>71,78,79</sup> However, the selectivity and affinity of CD320 and LDLR are very different: CD320 has the Cbl/TCN2 complex as its only natural ligand, whereas LDLR binds LDL but is not known to bind Cbl/TCN2. While LDLR-A1 and LDLR-A2 are present in both receptors, their spatial orientation in these receptors differs,<sup>62,80-82</sup> which is critical to ligand binding affinity and specificity. It is likely that, as with natural ligands, CD320 and LDLR display differences in binding to TCPP.

CD320 is not the only receptor through which TCPP enters the cell, since knockdown of CD320 protein did not result in a reduction of TCPP in every cancer cell line we tested. Moreover, in a panel of seven lung cancer cell lines, CD320 protein levels did not correlate with the ability to take up TCPP (Elzi and Rebel; unpublished observations). The reason for the variable effects of CD320 knockdown on TCPP uptake in the cell lines tested, even in series of the same tissue, is unknown. A likely possibility is that redundant receptors or transporters are present in the cell lines not affected by CD320 knockdown which can compensate for the loss of CD320 and facilitate TCPP entering into the cell. Candidate receptors to serve this redundancy role are the

import and export transporters of heme, a naturally occurring porphyrin.<sup>83-87</sup> Cancer cells often misregulate the expression of these transporters, resulting in an increased porphyrin uptake in cancer cells compared to normal cells.<sup>88,89</sup> Examples are SLC46A1 (HCP-1),<sup>83,88,90</sup> ABCB6,<sup>85,91</sup> and SLC48A1 (HRG-1).<sup>92</sup> Interestingly, while SLC46A1 and ABCB6 are expressed on the cell surface, SLC48A1 is normally expressed on the endosomal membrane; however, in cancer cells, SLC48A1 can be expressed on the plasma membrane and thereby facilitate porphyrin uptake.<sup>89</sup> Lastly, Kurokawa et al.<sup>93</sup> showed that the coordinated upregulation of the heme importer SLC46A1 and downregulation of the heme exporter ABCG2 resulted in porphyrin accumulation in cancer. In addition to the variety of receptors and transporters, the difference in TCPP uptake between cell lines might be a function of receptor/transporter expression levels, recycling, and or re-expression.

Further studies will be required to determine what other proteins are involved in the selective uptake of TCPP by cancer cells and how they relate to each other. The focus of our study was on the cancer cell itself. However, other porphyrins, such as padeliporfin (WST11), have been shown to localize to the tumor vascular tissue<sup>94</sup> while photofrin was taken up by tumor-associated macrophages.<sup>35,95</sup> Thus, the tumor microenvironment may play an important role in elucidating the tumor-localizing properties of TCPP. A more comprehensive understanding of interactions between specific porphyrins, cancer cells, and cancer-associated cells may help improve several oncology-related technologies, including the development of porphyrin-drug conjugates as highly specific drug-delivery vehicles for tumor tissue,<sup>96,97</sup> the use of porphyrins for the identification of tumor margins for surgical resection<sup>98</sup> and the development of improved porphyrins for cancer diagnostics.<sup>2</sup>

## ACKNOWLEDGMENTS

The authors thank Xiaojie Yu for assistance with some of the tissue culture experiments and David Rodriguez for assistance with the figure preparation.

## CONFLICT OF INTEREST

All authors were either employed or contracted by bioAffinity Technologies to perform the work described in this study.

## AUTHOR CONTRIBUTIONS

D. Elzi and V. Rebel were responsible for the overall execution of the project and wrote the manuscript. D. Elzi, W. Bauta, J. Sanchez, T. Das, S. Mogare, P. Fatland, and M. Iza designed and performed experiments. A. Pertsemidis contributed new reagents and analytical tools. D. Elzi, W. Bauta, J. Sanchez, A. Pertsemidis, and V. Rebel analyzed the data. All authors read and edited the paper to its final format.

## REFERENCES

- Rasmussen-Taxdal DS, Ward GE, Figge FHJ. Fluorescence of human lymphatic and cancer tissues following high doses of intravenous hematoporphyrin. *Cancer*. 1955;8:78-81.
- Patriquin L, Merrick DT, Hill D, et al. Early detection of lung cancer with meso tetra (4-carboxyphenyl) porphyrin-labeled sputum. *J Thorac Oncol*. 2015;10:1311-1318.
- Lange N, Jichlinski P, Zellweger M, et al. Photodetection of early human bladder cancer based on the fluorescence of 5-aminolaevulinic acid hexylester-induced protoporphyrin IX: a pilot study. *Br J Cancer*. 1999;80:185-193.
- Stenzl A, Burger M, Fradet Y, et al. Hexaminolevulinic acid guided fluorescence cystoscopy reduces recurrence in patients with non-muscle invasive bladder cancer. *J Urol*. 2010;184:1907-1914.
- Anand S, Ortel BJ, Pereira SP, Hasan T, Maytin EV. Biomodulatory approaches to photodynamic therapy for solid tumors. *Cancer Lett*. 2012;326:8-16.
- Azzouzi A-R, Vincendeau S, Barret E, et al. Padeliporfin vascular-targeted photodynamic therapy versus active surveillance in men with low-risk prostate cancer (CLIN1001 PCM301): an open-label, phase 3, randomised controlled trial. *Lancet Oncol*. 2017;18:181-191.
- Shafirstein G, Battoo A, Harris K, et al. Photodynamic therapy of non-small cell lung cancer. Narrative review and future directions. *Ann Am Thorac Soc*. 2016;13:265-275.
- Kessel D, Reiners J. Light-activated pharmaceuticals: mechanisms and detection. *Isr J Chem*. 2012;52:674-680.
- Cameron MC, Lee E, Hibler BP, et al. Basal cell carcinoma: contemporary approaches to diagnosis, treatment, and prevention. *J Am Acad Dermatol*. 2019;80:321-339.
- Kiesslich T, Neureiter D, Wolkersdörfer GW, Plaetzer K, Berr F. Advances in photodynamic therapy for the treatment of hilar biliary tract cancer. *Future Oncol*. 2010;6:1925-1936.
- Usuda J, Kato H, Okunaka T, et al. Photodynamic therapy (PDT) for lung cancers. *J Thorac Oncol*. 2006;1:489-493.
- Bredell MG, Besic E, Maake C, Walt H. The application and challenges of clinical PD-PDT in the head and neck region: a short review. *J Photochem Photobiol, B*. 2010;101:185-190.
- Cuenca RE, Allison RR, Sibata C, Downie GH. Breast cancer with chest wall progression: treatment with photodynamic therapy. *Ann Surg Oncol*. 2004;11:322-327.
- Wyss P, Schwarz V, Dobler-Girdziunaite D, et al. Photodynamic therapy of locoregional breast cancer recurrences using a chlorin-type photosensitizer. *Int J Cancer*. 2001;93:720-724.
- Mang TS, Allison R, Hewson G, Snider W, Moskowitz R. A phase II/III clinical study of tin ethyl etiopurpurin (Purlytin)-induced photodynamic therapy for the treatment of recurrent cutaneous metastatic breast cancer. *Cancer J Sci Am*. 1998;4:378-384.
- Kessel D. Porphyrin-lipoprotein association as a factor in porphyrin localization. *Cancer Lett*. 1986;33:183-188.
- Bonneau S, Vever-Bizet C, Morlière P, Mazière J-C, Brault D. Equilibrium and kinetic studies of the interactions of a porphyrin with low-density lipoproteins. *Biophys J*. 2002;83:3470-3481.
- Nakajima S, Takemura T, Sakata I. Tumor-localizing activity of porphyrin and its affinity to LDL, transferrin. *Cancer Lett*. 1995;92:113-118.
- Candide C, Morlière P, Mazière JC, et al. In vitro interaction of the photoactive anticancer porphyrin derivative photofrin II with low density lipoprotein, and its delivery to cultured human fibroblasts. *FEBS Lett*. 1986;207:133-138.
- Allison BA, Pritchard PH, Levy JG. Evidence for low-density lipoprotein receptor-mediated uptake of benzoporphyrin derivative. *Br J Cancer*. 1994;69:833-839.
- Shibata Y, Matsumura A, Yoshida F, et al. Competitive uptake of porphyrin and LDL via the LDL receptor in glioma cell lines: flow cytometric analysis. *Cancer Lett*. 2001;166:79-87.
- Silva JN, Filipe P, Morlière P, et al. Photodynamic therapies: principles and present medical applications. *Biomed Mater Eng*. 2006;16:S147-154.
- Mettlen M, Loerke D, Yarar D, Danuser G, Schmid SL. Cargo- and adaptor-specific mechanisms regulate clathrin-mediated endocytosis. *J Cell Biol*. 2010;188:919-933.
- Morris SM, Cooper JA. Disabled-2 colocalizes with the LDLR in clathrin-coated pits and interacts with AP-2. *Traffic*. 2001;2:111-123.
- Vitols S, Peterson C, Larsson O, Holm P, Åberg B. Elevated uptake of low density lipoproteins by human lung cancer tissue in vivo. *Cancer Res*. 1992;52:6244-6247.
- Beloribi-Djefaffia S, Vasseur S, Guillaumond F. Lipid metabolic reprogramming in cancer cells. *Oncogenesis*. 2016;5:e189.
- Mellman I, Yarden Y. Endocytosis and cancer. *Cold Spring Harb Perspect Biol*. 2013;5:a016949.
- Mosesson Y, Mills GB, Yarden Y. Derailed endocytosis: an emerging feature of cancer. *Nat Rev Cancer*. 2008;8:835-850.
- Schmitt F, Auzias M, Štěpnička P, et al. Sawhorse-type diruthenium tetracarbonyl complexes containing porphyrin-derived ligands as highly selective photosensitizers for female reproductive cancer cells. *J Biol Inorg Chem*. 2009;14:693-701.
- El-Far M, Pimstone N. A comparative study of 28 porphyrins and their abilities to localize in mammary mouse carcinoma: uroporphyrin I superior to hematoporphyrin derivative. *Prog Clin Biol Res*. 1984;170:661-672.
- Strauss WSL, Mohr W, Koenig K, Miller K, Rueck AC, Schneckenburger H, Steiner RW. Meso-tetra (4-carboxyphenyl) porphyrin-fluorescence behavior, photodynamic treatment, and tissue distribution. *SPIE*. 1994;2078:515-520. presented at the Photodynamic Therapy of Cancer.
- Cole, DA, Ellinwood, LE, Klein, MG. Method of using 5,10,15,20-tetrakis(carboxyphenyl)porphine for detecting cancers of the lung. U.S. Patent 3:597-875.
- Hu Z, Pan Y, Wang J, Chen J, Li J, Ren L. Meso-tetra (carboxyphenyl) porphyrin (TCPP) nanoparticles were internalized by SW480 cells by a clathrin-mediated endocytosis pathway to induce high photocytotoxicity. *Biomed Pharmacother*. 2009;63:155-164.
- Roberts WG, Hasan T. Role of neovasculature and vascular permeability on the tumor retention of photodynamic agents. *Cancer Res*. 1992;52:924-930.
- Korbelik M, Krosi G, Olive PL, Chaplin DJ. Distribution of photofrin between tumour cells and tumour associated macrophages. *Br J Cancer*. 1991;64:508-512.
- Kozyraki R, Cases O. Vitamin B12 absorption: mammalian physiology and acquired and inherited disorders. *Biochimie*. 2013;95:1002-1007.
- Quadros EV, Sequeira JM. Cellular uptake of cobalamin: transcobalamin and the TCbIR/CD320 receptor. *Biochimie*. 2013;95:1008-1018.
- Jiang W, Nakayama Y, Sequeira JM, Quadros EV. Characterizing monoclonal antibodies to antigenic domains of TCbIR/CD320,

- the receptor for cellular uptake of transcobalamin-bound cobalamin. *Drug Delivery*. 2011;18:74-78.
39. Xu M, Luo W, Elzi DJ, Grandori C, Galloway DA. NFX1 interacts with mSin3A/histone deacetylase to repress hTERT transcription in keratinocytes. *Mol Cell Biol*. 2008;28:4819-4828.
  40. Zimmer SN, Zhou Q, Zhou T, et al. Crebbp haploinsufficiency in mice alters the bone marrow microenvironment, leading to loss of stem cells and excessive myelopoiesis. *Blood*. 2011;118:69-79.
  41. Elkin SR, Bendris N, Reis CR, et al. A systematic analysis reveals heterogeneous changes in the endocytic activities of cancer cells. *Cancer Res*. 2015;75:4640-4650.
  42. Olsen JV, Ong S-E, Mann M. Trypsin cleaves exclusively C-terminal to arginine and lysine residues. *Mol Cell Proteomics*. 2004;3:608-614.
  43. Seltzer JL, Akers KT, Weingarten H, Grant GA, McCourt DW, Eisen AZ. Cleavage specificity of human skin type IV collagenase (gelatinase). Identification of cleavage sites in type I gelatin, with confirmation using synthetic peptides. *J Biol Chem*. 1990;265:20409-20413.
  44. Weimer S, Oertel K, Fuchsbauer H-L. A quenched fluorescent dipeptide for assaying dispase- and thermolysin-like proteases. *Anal Biochem*. 2006;352:110-119.
  45. Phillips RJ, Burdick MD, Hong K, et al. Circulating fibrocytes traffic to the lungs in response to CXCL12 and mediate fibrosis. *J Clin Invest*. 2004;114:438-446.
  46. Panchision DM, Chen H-L, Pistollato F, Papini D, Ni H-T, Hawley TS. Optimized flow cytometric analysis of central nervous system tissue reveals novel functional relationships among cells expressing CD133, CD15, and CD24. *Stem Cells*. 2007;25(6):1560-1570. <https://doi.org/10.1634/stemcells.2006-0260>
  47. Doherty GJ, McMahon HT. Mechanisms of endocytosis. *Annu Rev Biochem*. 2009;78:857-902.
  48. Dutta D, Donaldson JG. Search for inhibitors of endocytosis. *Cellular Logistics*. 2012;2:203-208.
  49. Iacopetta BJ, Morgan EH. The kinetics of transferrin endocytosis and iron uptake from transferrin in rabbit reticulocytes. *J Biol Chem*. 1983;258:9108-9115.
  50. Daniel JA, Chau N, Abdel-Hamid MK, et al. Phenothiazine-derived antipsychotic drugs inhibit dynamin and clathrin-mediated endocytosis. *Traffic*. 2015;16:635-654.
  51. Comisso C, Davidson SM, Soydaner-Azeloglu RG, et al. Macropinocytosis of protein is an amino acid supply route in Ras-transformed cells. *Nature*. 2013;497:633-637.
  52. Koivusalo M, Welch C, Hayashi H, et al. Amiloride inhibits macropinocytosis by lowering submembranous pH and preventing Rac1 and Cdc42 signaling. *J Cell Biol*. 2010;188:547-563.
  53. Sarkar K, Kruhlak MJ, Erlandsen SL, Shaw S. Selective inhibition by rottlerin of macropinocytosis in monocyte-derived dendritic cells. *Immunology*. 2005;116:513-524.
  54. An W, Jiao Y, Dong C, Yang C, Inoue Y, Shuang S. Spectroscopic and molecular modeling of the binding of meso-tetrakis(4-hydroxyphenyl)porphyrin to human serum albumin. *Dyes Pigm*. 2009;81:1-9.
  55. Andrade SM, Costa SMB. Spectroscopic studies on the interaction of a water soluble porphyrin and two drug carrier proteins. *Biophys J*. 2002;82:1607-1619.
  56. Aveline BM, Hasan T, Redmond RW. The effects of aggregation, protein binding and cellular incorporation on the photophysical properties of benzoporphyrin derivative monoacid ring A (BPDMA). *J Photochem Photobiol, B*. 1995;30:161-169.
  57. Bonneau S, Morlière P, Brault D. Dynamics of interactions of photosensitizers with lipoproteins and membrane-models: correlation with cellular incorporation and subcellular distribution. *Biochem Pharmacol*. 2004;68:1443-1452.
  58. Davila J, Harriman A. Photochemical and radiolytic oxidation of a zinc porphyrin bound to human serum albumin. *J Am Chem Soc*. 1990;112:2686-2690.
  59. Morgan WT, Alam J, Deaciuc V, Muster P, Tatum FM, Smith A. Interaction of hemopexin with Sn-protoporphyrin IX, an inhibitor of heme oxygenase. Role for hemopexin in hepatic uptake of Sn-protoporphyrin IX and induction of mRNA for heme oxygenase. *J Biol Chem*. 1988;263:8226-8231.
  60. Morgan WT, Smith A, Koskelo P. The interaction of human serum albumin and hemopexin with porphyrins. *Biochim Biophys Acta—Protein Struct*. 1980;624:271-285.
  61. Pasternack RF, Huber PR, Boyd P, et al. On the aggregation of meso-substituted water-soluble porphyrins. *J Am Chem Soc*. 1972;94:4511-4517.
  62. Alam A, Woo J-S, Schmitz J, et al. Structural basis of transcobalamin recognition by human CD320 receptor. *Nat Commun*. 2016;7:1-9.
  63. Jiang W, Nakayama Y, Sequeira JM, Quadros EV. Mapping the functional domains of TCbIR/CD320, the receptor for cellular uptake of transcobalamin-bound cobalamin. *FASEB J*. 2013;27:2988-2994.
  64. DiGirolamo PM, Huenekens FM. Transport of vitamin B12 into mouse leukemia cells. *Arch Biochem Biophys*. 1975;168:386-393.
  65. Radulescu AE, Siddhanta A, Shields D. A role for clathrin in re-assembly of the golgi apparatus. *Mol Biol Cell*. 2007;18:94-105.
  66. Royle SJ, Lagnado L. Clathrin-mediated endocytosis at the synaptic terminal: bridging the gap between physiology and molecules. *Traffic*. 2010;11:1489-1497.
  67. Dąbrowski JM, Pucelik B, Regiel-Futyra A, et al. Engineering of relevant photodynamic processes through structural modifications of metallotetrapyrrolic photosensitizers. *Coord Chem Rev*. 2016;325:67-101.
  68. Huang H, Chauhan S, Geng J, Qin Y, Watson DF, Lovell JF. Implantable tin porphyrin-PEG hydrogels with pH-responsive fluorescence. *Biomacromol*. 2017;18:562-567.
  69. Ravikant M, Reddy D, Chandrashekar TK. Dimerization effects on spectroscopic properties of water-soluble porphyrins in aqueous and micellar media. *J Chem Soc, Dalton Trans*. 1991;2103-2108.
  70. Kongshaug M, Moan J, Brown SB. The distribution of porphyrins with different tumour localising ability among human plasma proteins. *Br J Cancer*. 1989;59:184-188.
  71. Li L, Zhang X, Kovacic S, et al. Identification of a human follicular dendritic cell molecule that stimulates germinal center B cell growth. *J Exp Med*. 2000;191:1077-1084.
  72. Park HJ, Kim J-Y, Jung KI, Kim TJ. Characterization of a novel gene in the extended MHC region of mouse, NG29/Cd320, a homolog of the human CD320. *Immune Network*. 2009;9:138-146.
  73. Quadros EV, Nakayama Y, Sequeira JM. The protein and the gene encoding the receptor for the cellular uptake of transcobalamin-bound cobalamin. *Blood*. 2009;113:186-192.
  74. Amagasaki T, Green R, Jacobsen DW. Expression of transcobalamin II receptors by human leukemia K562 and HL-60 cells. *Blood*. 1990;76:1380-1386.
  75. Kirsch SH, Herrmann W, Obeid R. Genetic defects in folate and cobalamin pathways affecting the brain. *Clin Chem Lab Med*. 2012;51:139-155.

76. Quadros EV, Nakayama Y, Sequeira JM. Saporin conjugated monoclonal antibody to the transcobalamin receptor TCbIR/CD320 is effective in targeting and destroying cancer cells. *J Cancer Ther.* 2013;4:1074-1081.
77. Pollard TD. A guide to simple and informative binding assays. *MBoC.* 2010;21:4061-4067.
78. Martínez-Oliván J, Rozado-Aguirre Z, Arias-Moreno X, Angarica VE, Velázquez-Campoy A, Sancho J. Low-density lipoprotein receptor is a calcium/magnesium sensor—role of LR4 and LR5 ion interaction kinetics in low-density lipoprotein release in the endosome. *FEBS J.* 2014;281:2638-2658.
79. Martínez-Oliván J, Arias-Moreno X, Hurtado-Guerrero R, et al. The closed conformation of the LDL receptor is destabilized by the low Ca(++) concentration but favored by the high Mg(++) concentration in the endosome. *FEBS Lett.* 2015;589:3534-3540.
80. Beglova N, Blacklow SC. The LDL receptor: how acid pulls the trigger. *Trends Biochem Sci.* 2005;30:309-317.
81. Beglova N, Jeon H, Fisher C, Blacklow SC. Cooperation between fixed and low pH-inducible interfaces controls lipoprotein release by the LDL receptor. *Mol Cell.* 2004;16:281-292.
82. Rudenko G, Henry L, Henderson K, et al. Structure of the LDL receptor extracellular domain at endosomal pH. *Science.* 2002;298:2353-2358.
83. Hiyama K, Matsui H, Tamura M, et al. Cancer cells uptake porphyrins via heme carrier protein 1. *J Porphyrins Phthalocyanines.* 2012;17:36-43.
84. Boswell-Casteel RC, Fukuda Y, Schuetz JD. ABCB6, an ABC transporter impacting drug response and disease. *AAPS J.* 2017;20:8.
85. Zhao S-G, Chen X-F, Wang L-G, et al. Increased expression of ABCB6 enhances protoporphyrin ix accumulation and photodynamic effect in human glioma. *Ann Surg Oncol.* 2013;20:4379-4388.
86. Kim JH, Park JM, Roh YJ, Kim I-W, Hasan T, Choi M-G. Enhanced efficacy of photodynamic therapy by inhibiting ABCG2 in colon cancers. *BMC Cancer.* 2015;15:504.
87. Khot MI, Downey CL, Armstrong G, et al. The role of ABCG2 in modulating responses to anti-cancer photodynamic therapy. *Photodiagn Photodyn Ther.* 2020;29:101579.
88. Hooda J, Cadinu D, Alam MM, et al. Enhanced heme function and mitochondrial respiration promote the progression of lung cancer cells. *PLoS One.* 2013;8:e63402.
89. Fogarty FM, O'Keeffe J, Zhadanov A, Papkovsky D, Ayllon V, O'Connor R. HRG-1 enhances cancer cell invasive potential and couples glucose metabolism to cytosolic/extracellular pH gradient regulation by the vacuolar-H+ ATPase. *Oncogene.* 2014;33:4653-4663.
90. Takada T, Tamura M, Yamamoto T, Matsui H, Matsumura A. Selective accumulation of hematoporphyrin derivative in glioma through proton-coupled folate transporter SLC46A1. *J Clin Biochem Nutr.* 2014;54:26-30.
91. Nakayama T, Otsuka S, Kobayashi T, et al. Dormant cancer cells accumulate high protoporphyrin IX levels and are sensitive to 5-aminolevulinic acid-based photodynamic therapy. *Sci Rep.* 2016;6:36478.
92. O'Callaghan KM, Ayllon V, O'Keeffe J, et al. Heme-binding protein HRG-1 Is induced by insulin-like growth factor I and associates with the vacuolar H+-ATPase to control endosomal pH and receptor trafficking. *J Biol Chem.* 2010;285:381-391.
93. Kurokawa H, Ito H, Terasaki M, Matsui H. Hyperthermia enhances photodynamic therapy by regulation of HCP1 and ABCG2 expressions via high level ROS generation. *Sci Rep.* 2019;9:1638.
94. Mazor O, Brandis A, Plaks V, et al. WST11, a novel water-soluble bacteriochlorophyll derivative; cellular uptake, pharmacokinetics, biodistribution and vascular-targeted photodynamic activity using melanoma tumors as a model. *Photochem Photobiol.* 2005;81:342-351.
95. Korbelik M, Krosli G, Chaplin DJ. Photofrin uptake by murine macrophages. *Cancer Res.* 1991;51:2251-2255.
96. Mittal S, Bhadwal M, Das T, et al. Synthesis and biological evaluation of 90Y-labeled porphyrin-DOTA conjugate: a potential molecule for targeted tumor therapy. *Cancer Biother Radiopharm.* 2013;28:651-656.
97. Shi J, Liu TWB, Chen J, et al. Transforming a targeted porphyrin theranostic agent into a PET imaging probe for cancer. *Theranostics.* 2011;1:363-370.
98. Piffaretti D, Burgio F, Thelen M, et al. Protoporphyrin IX tracer fluorescence modulation for improved brain tumor cell lines visualization. *J Photochem Photobiol, B.* 2019;201:111640.
99. Harrison SM, Bers DM. The effect of temperature and ionic strength on the apparent Ca-affinity of EGTA and the analogous Ca-chelators BAPTA and dibromo-BAPTA. *Biochim Biophys Acta—Gen Subj.* 1987;925:133-143.
100. Matsuda S, Yagi K. The apparent binding constants of Ca2+ to EGTA and heavy meromyosin1. *J Biochem.* 1980;88:1515-1520.

## SUPPORTING INFORMATION

Additional Supporting Information may be found online in the Supporting Information section.

**How to cite this article:** Elzi DJ, Bauta WE, Sanchez JR, et al. Identification of a novel mechanism for meso-tetra (4-carboxyphenyl) porphyrin (TCPP) uptake in cancer cells. *The FASEB Journal.* 2021;35:e21427. <https://doi.org/10.1096/fj.202000197R>